

# Interplay of nonclassicality and entanglement of two-mode Gaussian fields generated in optical parametric processes

Ievgen I. Arkhipov\*

*RCPTM, Joint Laboratory of Optics of Palacký University and Institute of Physics of CAS,  
Palacký University, 17. listopadu 12, 771 46 Olomouc, Czech Republic*

Jan Peřina Jr.

*Joint Laboratory of Optics of Palacký University and Institute of Physics of CAS,  
Institute of Physics of the Czech Academy of Science,  
17. listopadu 50a, 771 46 Olomouc, Czech Republic*

Jan Peřina

*Joint Laboratory of Optics of Palacký University and Institute of Physics of CAS,  
Palacký University, 17. listopadu 12, 771 46 Olomouc, Czech Republic*

Adam Miranowicz

*Faculty of Physics, Adam Mickiewicz University, PL-61-614 Poznań, Poland*

The behavior of general nonclassical two-mode Gaussian states at a beam splitter is investigated. Single-mode nonclassicality as well as two-mode entanglement of both input and output states are analyzed suggesting their suitable quantifiers. These quantifiers are derived from local and global invariants of linear unitary two-mode transformations such that the sum of input (or output) local nonclassicality measures and entanglement measure gives a global invariant. This invariant quantifies the global nonclassicality resource. Mutual transformations of local nonclassicalities and entanglement induced by the beam splitter are analyzed considering incident noisy twin beams, single-mode noisy squeezed vacuum states, and states encompassing both squeezed states and twin beams. A rich tapestry of interesting nonclassical output states is predicted.

PACS numbers: 42.65.Lm, 42.50.Ar, 03.67.Mn, 42.65.Yj

## I. INTRODUCTION

The nonclassical properties of light have been for a long time the main topic of interest in quantum optics. The question whether a given quantum state is nonclassical (i.e., cannot be treated by the classical statistical theory) has been considered as one of the most important problems since the early days of quantum physics [1–3] (for a review see, e.g., Refs. [4–6]). For optical fields, a commonly accepted criterion for distinguishing nonclassical states from the classical ones is expressed as follows [5, 7–9]: a quantum state is nonclassical if its Glauber-Sudarshan  $P$  function fails to have all the properties of a probability density. We recall that the Glauber-Sudarshan  $P$  function for an  $M$ -mode bosonic state  $\hat{\rho}$  can be defined as [10, 11]:

$$\hat{\rho} = \int P(\boldsymbol{\alpha}, \boldsymbol{\alpha}^*) |\boldsymbol{\alpha}\rangle \langle \boldsymbol{\alpha}| d^2\boldsymbol{\alpha}, \quad (1)$$

where  $|\boldsymbol{\alpha}\rangle = \prod_{m=1}^M |\alpha_m\rangle$  is given in terms of the  $m$ th-mode coherent state  $|\alpha_m\rangle$ , which is the eigenstate of the  $m$ th-mode annihilation operator  $\hat{a}_m$ ,  $\boldsymbol{\alpha}$  denotes complex multivariable  $(\alpha_1, \alpha_2, \dots, \alpha_M)$ , and  $d^2\boldsymbol{\alpha} = \prod_m d^2\alpha_m$ . It is worth noting that the negativity of the  $P$  function

is necessary and sufficient for nonclassicality, while the singularity or irregularity of the  $P$  function is only a sufficient condition (i.e., it is a nonclassical witness). Thus, if the  $P$  function is more singular or more irregular than Dirac's  $\delta$ -function for a given state, then it is also non-positive (semidefinite) in the formalism of generalized functions. A standard example of such irregular functions is the  $P$  function for an  $n$ -photon Fock state (with  $n = 1, 2, \dots$ ), which is given by the  $n$ th derivative of  $\delta(\boldsymbol{\alpha})$ .

Based on this definition of nonclassicality, various operational criteria (also called witnesses) have been described for testing the nonclassicality of single-mode [7, 8, 12] and multi-mode [13–15] fields. Their derivations are based either on the fields moments [13, 15, 16] or exploit the Bochner theorem written for the characteristic function of the Glauber-Sudarshan  $P$  function [17]. A direct reconstruction of the quasi-distributions of integrated intensities is a sufficient but not necessary condition of the nonclassicality of the detected fields by the definition [18–20]. We note that nonclassicality criteria derived from the majorization theory have also been found useful [21, 22].

Entanglement between two optical fields is one of the most frequently studied forms of nonclassical light. Such light emerges in various two-mode or multimode nonlinear optical processes, e.g., in spontaneous parametric down-conversion. In this process, pairs of photons composed of the signal and idler modes are created at the

\* ievgen.arkhipov01@upol.cz

expense of the annihilated pump photons. This pairwise character of emitted light lies in the heart of entanglement here. The process of spontaneous parametric down-conversion has its degenerate variant called second-subharmonic generation, where both photons in a pair are emitted into the same optical mode. This gives rise to phase squeezing of the second-subharmonic field composed of, in general, many photon pairs. The squeezed light is also considered nonclassical as it has its phase fluctuations suppressed below the classical limit. The nonclassicality in both cases has the same origin which is pairing of photons. On the other side, the emitted photon pairs can be manipulated by linear optics. In detail, two photons from one pair present in the same mode of a squeezed state of light can be split (on a beam splitter) and contribute to the entanglement of the output fields. Also, two photons from a pair incident on different input ports of a beam splitter can “stick together” (bunch) and leave the beam splitter in the same output port (as testified in the Hong-Ou-Mandel interferometer [23]). The interconnection of these two types of fields by the means of linear optics has already been shown by Braunstein [24] and later elaborated by Adesso [25] for arbitrarily strong Gaussian states. This behavior poses a natural question whether it is possible to introduce a physical quantity that quantifies “a nonclassicality resource” present during the creation of both types of fields and later conserved during linear-optical transformations.

The answer to this question is intimately related to the quantifiers of *entanglement* and *local nonclassicality*. Several measures were proposed to quantify the entanglement in both discrete and continuous domains [26–31]. The negativity (or its logarithmic variant) is considered, probably, as the most useful at present. On the other hand, the Lee nonclassicality depth [21] is conventionally used to quantify the nonclassicality of optical fields. Alternatively, the nonclassicality of an optical field can be transcribed to entanglement using a beam splitter and quantified via an entanglement measure [32, 33]. For a comparative study of these two nonclassicality measures see, e.g., recent Refs. [34, 35].

We note that, apart from the local nonclassicalities of two parts of a bipartite state, also *global nonclassicality* can naturally be defined. All these three quantities have been analyzed in Ref. [36] for intense multi-mode twin beams with the following result: whenever a twin beam is entangled it is globally nonclassical. On the other hand, its signal and idler constituents are multi-thermal and so locally classical. A general approach for describing the relation between the entanglement and global nonclassicality of two-mode states has been proposed in Ref. [37].

Returning back to our question, we look for an invariant with respect to linear-unitary transformations (conserving the overall number of photons) that comprises both the entanglement and local nonclassicalities. This question has recently been addressed in Ref. [38] considering beam-splitter transformations and a quantity composed of the logarithmic negativity and the logarithm

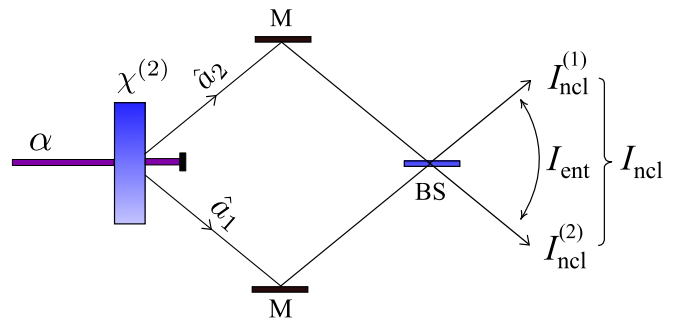


FIG. 1. (Color online) Diagram showing the main goal of this paper: The local ( $I_{\text{ncl}}^{(1)}$  and  $I_{\text{ncl}}^{(2)}$ ) and global ( $I_{\text{ncl}}$ ) nonclassicality invariants are analyzed in relation with the entanglement, described by the invariant  $I_{\text{ent}}$ , for the light generated by the optical parametric process (described by the second-order susceptibility  $\chi^{(2)}$ ) and then combined at a beam splitter BS with varying transmissivity  $T$ . Here,  $\alpha$  is the amplitude of a classical pump field,  $\hat{a}_1$  and  $\hat{a}_2$  are the annihilation operators of the generated light, and  $M$  denotes a mirror.

of nonclassicality depth. However, the introduced quantity has been found useful only under very specific conditions [39].

In this paper we construct such an invariant for general two-mode Gaussian states arising in nonlinear processes described by the second order susceptibility  $\chi^{(2)}$ . The processes of spontaneous parametric down-conversion and second-subharmonic generation represent their most important examples. As schematically shown in Fig. 1, the found invariant is decomposable into three parts characterizing in turn entanglement and two local nonclassicalities. The entanglement indicator is shown to be a monotone of the logarithmic negativity similarly to the newly defined nonclassicality measure that is a monotone of the Lee nonclassicality depth under any linear unitary transformation.

The obtained results are potentially interesting for manipulations with nonclassicality in quantum engineering that have become substantial ingredients of a growing number of applications of quantum technologies [28, 40–43].

The paper is organized as follows. In Sec. II, a model comprising parametric down-conversion and second-subharmonic generation is developed. A suitable nonclassicality invariant is suggested using local and global invariants of two-mode Gaussian fields. Its decomposition into an entanglement quantifier and local nonclassicality quantifiers is also discussed. Twin beams as they behave on a beam splitter are discussed in Sec. III. In Sec. IV, a single-mode squeezed state on a beam splitter is analyzed. Section V is devoted to the behavior of two single-mode squeezed states interfering on a beam splitter. States having both ‘twin-beam’ and squeezed components are investigated in Sec. VI. Conclusions are drawn in Sec. VII. Quasidistributions related to the normal and symmetric ordering of operators are discussed in the Appendix.

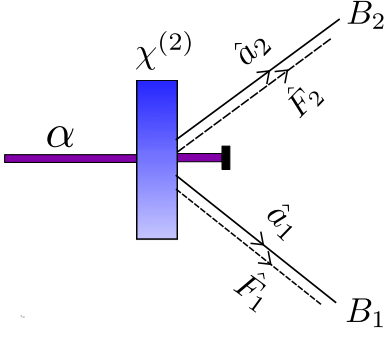


FIG. 2. (Color online) Diagram of the optical parametric process described by Eq. (2): the classical pump field, with complex amplitude  $\alpha$ , generates the signal and idler modes described by the annihilation operators  $\hat{a}_j$  and affected by the noise stochastic operators  $\hat{F}_j$ ,  $j = 1, 2$ . For simplicity, the pump-field amplitude  $\alpha$  is incorporated into the coupling constants  $g_{ij}$ . The mean photon number in the signal (idler) mode influenced by the noise is denoted by  $B_1$  ( $B_2$ ). In Sec. III,  $B_1 = B_p + B_s$  and  $B_2 = B_p + B_i$ , where  $B_p = \sinh^2(g_{12}t)$  is the mean number of generated photon pairs and  $B_s = \langle \hat{F}_1^\dagger \hat{F}_1 \rangle$  ( $B_i = \langle \hat{F}_2^\dagger \hat{F}_2 \rangle$ ) is the mean number of signal (idler) noise photons. In Secs. IV and V,  $B_1 = \hat{B}_p^s + B_s$  and  $B_2 = \hat{B}_p^i + B_i$ , where  $\hat{B}_p^s$  ( $\hat{B}_p^i$ ) is the mean number of squeezed photons in the signal (idler) mode.

## II. GAUSSIAN STATES GENERATED IN $\chi^{(2)}$ INTERACTIONS AND THEIR INVARIANTS

We consider a nonlinear interaction Hamiltonian  $\hat{H}_{\text{int}}$  describing both parametric down-conversion and second-subharmonic generation that provide photon pairs [9] (for the scheme, see Fig. 2):

$$\hat{H}_{\text{int}} = -\hbar g_{12}^* \hat{a}_1 \hat{a}_2 - \hbar g_{11}^* \hat{a}_1^2 - \hbar g_{22}^* \hat{a}_2^2 + \text{h.c.} \quad (2)$$

In Eq. (2), the symbols  $\hat{a}_1$  ( $\hat{a}_1^\dagger$ ) and  $\hat{a}_2$  ( $\hat{a}_2^\dagger$ ) represent the annihilation (creation) operators of the fields 1 and 2,  $g_{12}$  is a nonlinear coupling constant characterizing parametric down-conversion and  $g_{ii}$  stands for a nonlinear coupling constant of the second-subharmonic generation in the  $i$ th mode described by the second-order susceptibility  $\chi^{(2)}$  of a medium. Symbol h.c. represents the Hermitian conjugated terms. Due to the presence of noise in real nonlinear processes we also consider the Langevin forces  $\hat{L}_j$  arising in the interaction with the reservoir chaotic oscillators characterized by means of noise photon numbers  $\langle n_d \rangle$ . This leads to damping processes described by the damping constants  $\gamma_j$ .

The Heisenberg-Langevin operator equations corresponding to the Hamiltonian  $\hat{H}_{\text{int}}$  are derived in the following matrix form:

$$\frac{d\hat{\mathbf{a}}}{dt} = \mathbf{M}\hat{\mathbf{a}} + \hat{\mathbf{L}} \quad (3)$$

using the vectors  $\hat{\mathbf{a}} = (\hat{a}_1, \hat{a}_1^\dagger, \hat{a}_2, \hat{a}_2^\dagger)^T$  and  $\hat{\mathbf{L}} =$

$(\hat{L}_1, \hat{L}_1^\dagger, \hat{L}_2, \hat{L}_2^\dagger)^T$ , and the matrix

$$\mathbf{M} = \begin{bmatrix} -\gamma_1/2 & 2ig_{11} & 0 & ig_{12} \\ -2ig_{11} & -\gamma_1/2 & -ig_{12} & 0 \\ 0 & ig_{12} & -\gamma_2/2 & 2ig_{22} \\ -ig_{12} & 0 & -2ig_{22} & -\gamma_2/2 \end{bmatrix}. \quad (4)$$

The Langevin operators  $\hat{L}_1$  and  $\hat{L}_2$  introduced in Eq. (3) obey the following relations:

$$\begin{aligned} \langle \hat{L}_i(t) \rangle &= \langle \hat{L}_i^\dagger(t) \rangle = 0, \\ \langle \hat{L}_i^\dagger(t) \hat{L}_j(t') \rangle &= \delta_{ij} \langle n_d \rangle \delta(t - t'), \\ \langle \hat{L}_i(t) \hat{L}_j^\dagger(t') \rangle &= \delta_{ij} (\langle n_d \rangle + 1) \delta(t - t'), \end{aligned} \quad (5)$$

where  $\delta_{ij}$  stands for the Kronecker symbol and  $\delta$  denotes the Dirac delta function.

The solution of Eq. (3) for the operators  $\hat{a}_1$  and  $\hat{a}_2$  is conveniently written in the following matrix form using suitable evolution matrices  $\mathbf{U}$  and  $\mathbf{V}$  and a stochastic operator vector  $\hat{\mathbf{F}}$  (for details, see, e.g. [44]):

$$\begin{bmatrix} \hat{a}_1(t) \\ \hat{a}_2(t) \end{bmatrix} = \mathbf{U}(t) \begin{bmatrix} \hat{a}_1(0) \\ \hat{a}_2(0) \end{bmatrix} + \mathbf{V}(t) \begin{bmatrix} \hat{a}_1^\dagger(0) \\ \hat{a}_2^\dagger(0) \end{bmatrix} + \hat{\mathbf{F}}(t). \quad (6)$$

Specific forms of the general evolution matrices  $\mathbf{U}$  and  $\mathbf{V}$  are discussed in the sections below. The elements of the stochastic operator vector  $\hat{\mathbf{F}} \equiv (\hat{F}_1, \hat{F}_2)$  are derived as linear combinations of the Langevin forces  $\hat{L}_j$  and  $\hat{L}_j^\dagger$  that reflect the ‘deterministic’ solution described by the matrices  $\mathbf{U}$  and  $\mathbf{V}$  [44].

Statistical properties of the emitted fields, in a given state  $\hat{\rho}$ , are described by the Glauber-Sudarshan  $P$  function, given by Eq. (1), or, equivalently, by the normal quantum characteristic function  $C_{\mathcal{N}}$  defined as

$$C_{\mathcal{N}}(\beta_1, \beta_2) = \left\langle \exp(\beta_1 \hat{a}_1^\dagger + \beta_2 \hat{a}_2^\dagger) \exp(-\beta_1^* \hat{a}_1 - \beta_2^* \hat{a}_2) \right\rangle, \quad (7)$$

where symbol  $\langle \dots \rangle$  denotes quantum averaging including both system and reservoir. Using the solution given in Eq. (6) and the initial vacuum states in both fields, the normal characteristic function  $C_{\mathcal{N}}$  attains the following form:

$$C_{\mathcal{N}}(\beta_1, \beta_2) = \exp \left[ -B_1 |\beta_1|^2 - B_2 |\beta_2|^2 + \left( \frac{C_1}{2} \beta_1^{*2} + \frac{C_2}{2} \beta_2^{*2} + D_{12} \beta_1^* \beta_2^* + \bar{D}_{12} \beta_1 \beta_2 + \text{c.c.} \right) \right], \quad (8)$$

where the auxiliary functions are defined as follows:

$$\begin{aligned} B_j &= \langle \Delta \hat{a}_j^\dagger \Delta \hat{a}_j \rangle = \sum_{k=1,2} |V_{jk}|^2 + \langle \hat{F}_j^\dagger \hat{F}_j \rangle, \\ C_j &= \langle (\Delta \hat{a}_j)^2 \rangle = \sum_{k=1,2} U_{jk} V_{jk} + \langle \hat{F}_j^2 \rangle, \\ D_{12} &= \langle \Delta \hat{a}_1 \Delta \hat{a}_2 \rangle = \sum_{k=1,2} U_{1k} V_{2k} + \langle \hat{F}_1 \hat{F}_2 \rangle, \\ \bar{D}_{12} &= -\langle \Delta \hat{a}_1^\dagger \Delta \hat{a}_2 \rangle = -\sum_{k=1,2} V_{1k}^* V_{2k} - \langle \hat{F}_1^\dagger \hat{F}_2 \rangle. \end{aligned} \quad (9)$$

Ordering	Quasidistribution	Characteristic function	Covariance matrix of a Gaussian state
Normal	$P(\alpha_1, \alpha_2) \equiv W^{(s=1)}(\alpha_1, \alpha_2) \iff$	$C_N(\beta_1, \beta_2) \longleftrightarrow$	$A_N$
	$\Downarrow \Uparrow$	$\Downarrow \Uparrow$	$\Downarrow \Uparrow$
Symmetric	$W(\alpha_1, \alpha_2) \equiv W^{(s=0)}(\alpha_1, \alpha_2) \iff$	$C_S(\beta_1, \beta_2) \longleftrightarrow$	$A_S$

TABLE I. Schematic diagram for the relations between (a) two quasiprobability distributions (quasidistributions), i.e., the Glauber-Sudarshan  $P$  and Wigner  $W$  functions for a given two-mode state  $\hat{\rho}$ , (b) characteristic functions  $C_N$  and  $C_S$ , and (c) covariance matrices  $A_N$  and  $A_S$  assuming here that  $\hat{\rho}$  is a Gaussian state for normal and symmetric orderings, respectively. Their interrelations (as marked by left-right arrows) are given in Appendix A. The single arrow indicates that the calculation of the  $P$  function from the Wigner function is more complicated (it can be done via the relation between  $C_S$  and  $C_N$ ) than the trivial calculation of the Wigner function from the  $P$  function (as marked by double arrow).

The normal characteristic function given in Eq. (8) can conveniently be rewritten into its matrix form  $C_N(\beta) = \exp(\beta^\dagger \mathbf{A}_N \beta / 2)$  using the covariance matrix  $\mathbf{A}_N$  related to the normal ordering [45] (for different possibilities in describing the generated fields, see Table I):

$$\mathbf{A}_N = \begin{bmatrix} -B_1 & C_1 & \bar{D}_{12}^* & D_{12} \\ C_1^* & -B_1 & D_{12}^* & \bar{D}_{12} \\ \bar{D}_{12} & D_{12} & -B_2 & C_2 \\ D_{12}^* & \bar{D}_{12}^* & C_2^* & -B_2 \end{bmatrix}, \quad (10)$$

and the column vector  $\beta = (\beta_1, \beta_1^*, \beta_2, \beta_2^*)^T$ .

The covariance matrix  $\mathbf{A}_N$  related to the normal ordering determines the *global nonclassicality* of a two-mode Gaussian state via the Lee nonclassicality depth  $\tau$ . The nonclassicality depth  $\tau$  is defined with the help of the maximal positive eigenvalue  $\lambda_+(\mathbf{A}_N)$  of the matrix  $\mathbf{A}_N$  as follows:

$$\tau = \max[0, \lambda_+(\mathbf{A}_N)]. \quad (11)$$

We note that the nonclassicality depth  $\tau$ , according to its definition [21], gives the amount of noise photons present equally in both modes and needed to conceal the nonclassical character of the state.

The covariance matrix  $\mathbf{A}_N$  of the two-mode field can be written in the following block form:

$$\begin{aligned} \mathbf{A}_N &= \begin{bmatrix} \mathbf{B}_1 & \mathbf{D}_{12} \\ \mathbf{D}_{21} & \mathbf{B}_2 \end{bmatrix}, \\ \mathbf{B}_j &= \begin{bmatrix} -B_j & C_j \\ C_j^* & -B_j \end{bmatrix}, \quad j = 1, 2, \\ \mathbf{D}_{12} &= \begin{bmatrix} \bar{D}_{12}^* & D_{12} \\ D_{12}^* & \bar{D}_{12} \end{bmatrix}, \\ \mathbf{D}_{21} &= \begin{bmatrix} \bar{D}_{12} & D_{12} \\ D_{12}^* & \bar{D}_{12}^* \end{bmatrix}. \end{aligned} \quad (12)$$

This form points out at the existence of three local invariants  $I_j$ ,  $j = 1, 2, 3$ , that do not change under any

local linear unitary transformation applied in mode 1 or 2. The local invariants  $I_j$  are expressed as:

$$I_1 = \det(\mathbf{B}_1), \quad I_2 = \det(\mathbf{B}_2), \quad I_3 = \det(\mathbf{D}_{12}). \quad (13)$$

Moreover, there exist two global invariants  $I$  and  $\Delta$  preserved under arbitrary linear unitary transformations and applied to both modes:

$$I = \det(\mathbf{A}_N), \quad \Delta = I_1 + I_2 + 2I_3. \quad (14)$$

Whereas the global invariant  $I$  encompasses the whole complex structure of the matrix  $\mathbf{A}_N$  and, as such, is not useful in our considerations, the global invariant  $\Delta$  reflects the block structure of the matrix  $\mathbf{A}_N$  and lies in the center of our attention.

Moreover, the global invariant  $\Delta$  includes the additive local invariants  $I_1$  and  $I_2$  that indicate the nonclassical behavior of the reduced states of modes 1 and 2, respectively. Indeed, the determinants defining these invariants occur in the Fourier transform of the normal characteristic functions of the reduced states directly related to their local Glauber-Sudarshan  $P$  functions. If a determinant fails to be positive then the corresponding Glauber-Sudarshan  $P$  function does not exist as a nonnegative function. Thus, the value of determinant  $I_j$  can be used to quantify the *local nonclassicality* of the reduced state in mode  $j$  as it is a monotone of the local Lee nonclassicality depth  $\tau_j$ . The local Lee nonclassicality depth  $\tau_j$  is defined along the formula (11) that provides the relation:

$$\tau_j = \max(0, |C_j| - B_j), \quad j = 1, 2. \quad (15)$$

Using Eq. (15) we arrive at the monotonic relation between the local nonclassicality depth  $\tau_j$  and local nonclassicality invariant (NI)  $I_j$  if we assume  $\tau_j$  to be continuous:

$$I_j = -\tau_j (\tau_j + 2B_j). \quad (16)$$

We can redefine the local symplectic invariant in Eq. (16) as  $I_{\text{ncl}}^{(j)} = -I_j$  in order to deal with positive values when quantifying the local nonclassicality. We note that not

only the positive values of this local NI  $I_{\text{ncl}}^{(1)}$  are useful for quantifying the local nonclassicality, also the negative values of this invariant are important as they quantify the “robustness” of the classicality of a local state.

Returning back to the last term  $I_3$  in the global invariant  $\Delta$ , this term describes solely the mutual quantum correlations between the fields 1 and 2. As such, it has to play a crucial role in the description of the entanglement between two fields. To reveal and quantify this entanglement and the role of local invariant  $I_3$  here, we apply for a while the phase space  $(x, p)$  approach for describing the fields in the symmetric ordering of field operators corresponding to the Wigner formalism (see Table 1 and then the Appendix). The reason is technical and is given by the fact that we know how to derive the covariance matrix of a Gaussian state obtained by the partial transposition of the original state. According to Simon [46], the partial transposition means to replace  $p$  by  $-p$ . The covariance matrix of the partially transposed state then provides us the logarithmic negativity  $E_N$  that is a commonly used measure for the entanglement. Moreover, it provides as an entanglement measure useful in our considerations.

In detail, the covariance matrix  $\mathbf{A}_S$  expressed in the symmetric ordering is obtained in its block structure as follows:

$$\mathbf{A}_S = \begin{bmatrix} \mathbf{B}_{S1} & \mathbf{D}_S \\ \mathbf{D}_S^T & \mathbf{B}_{S2} \end{bmatrix}, \quad (17)$$

$$\mathbf{B}_{Sj} = \begin{bmatrix} B_j + \text{Re}(C_j) + 1/2 & \text{Im}(C_j) \\ \text{Im}(C_j) & B_j - \text{Re}(C_j) + 1/2 \end{bmatrix}, \quad j = 1, 2,$$

$$\mathbf{D}_S = \begin{bmatrix} \text{Re}(D_{12} - \bar{D}_{12}) & \text{Im}(D_{12} + \bar{D}_{12}) \\ \text{Im}(D_{12} - \bar{D}_{12}) & -\text{Re}(D_{12} + \bar{D}_{12}) \end{bmatrix}.$$

The covariance matrix  $\mathbf{A}_S$ , similarly as its normally-ordered counterpart, has three local invariants  $I_{Sj}$ ,  $j = 1, 2, 3$ , and two global ones denoted as  $I_S$  and  $\Delta_S$ :

$$I_{S1} = \det(\mathbf{B}_{S1}), \quad I_{S2} = \det(\mathbf{B}_{S2}), \quad I_{S3} = \det(\mathbf{D}_S), \\ I_S = \det(\mathbf{A}_S), \quad \Delta_S = I_{S1} + I_{S2} + 2I_{S3}. \quad (18)$$

Moreover, the comparison of the formulas for the invariants  $I_3$  and  $I_{S3}$  shows that  $I_3 = I_{S3}$ .

Following Refs. [31, 46, 47], the entanglement criterion can be expressed through the positivity of the entanglement indicator (EI)  $I_{\text{ent}}$  defined in terms of the invariants in Eq. (18) as follows:

$$I_{\text{ent}} = \frac{1}{4}(I_{S1} + I_{S2} - 2I_{S3}) - I_S - \frac{1}{16}. \quad (19)$$

As we show below the EI  $I_{\text{ent}}$  is a monotonous function of logarithmic negativity  $E_N$ , which can be derived from the symplectic eigenvalue  $\tilde{d}_-$  of the partially transposed (PT) matrix  $\mathbf{A}_S^{\text{PT}}$  along the formula [48] (see Fig. 3)

$$E_N = \max[0, -\ln(2\tilde{d}_-)]. \quad (20)$$

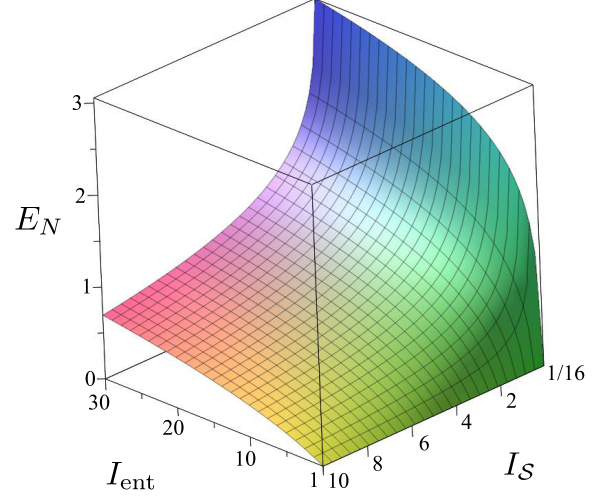


FIG. 3. (Color online) Logarithmic negativity  $E_N$  as a function of entanglement indicator  $I_{\text{ent}}$ , given by Eq. (19), and global nonclassicality invariant  $I_S$ , given by Eq. (18).

According to Eq. (20), a state is entangled if  $\tilde{d}_- < 1/2$ . In turn, the symplectic eigenvalue  $\tilde{d}_-$  is found as:

$$\tilde{d}_- = \frac{1}{\sqrt{2}} \sqrt{\tilde{\Delta}_S - \sqrt{\tilde{\Delta}_S^2 - 4I_S}}, \quad (21)$$

where  $\tilde{\Delta}_S = I_{S1} + I_{S2} - 2I_{S3}$ . Combining Eqs. (19) and (21) we arrive at the relation between the symplectic eigenvalue  $\tilde{d}_-$  and entanglement indicator  $I_{\text{ent}}$ :

$$\tilde{d}_- = \frac{1}{\sqrt{2}} \sqrt{I' - \sqrt{I'^2 - 4I_S}}, \quad (22)$$

where  $I' = 4I_S + 4I_{\text{ent}} + \frac{1}{4}$ .

Assuming the global invariant  $I_S$  is fixed, the relation (22) shows that the larger is the entanglement indicator  $I_{\text{ent}}$ , the smaller is the symplectic eigenvalue  $\tilde{d}_-$  and, according to formula (20), also the larger is the logarithmic negativity  $E_N$ . As a consequence, the entanglement indicator  $I_{\text{ent}}$  represents an alternative to the logarithmic negativity  $E_N$  in quantifying entanglement. We illustrate the monotonous dependence of the logarithmic negativity  $E_N$  on the entanglement indicator  $I_{\text{ent}}$  in Fig. 2. We note that a simple analytical formula between the logarithmic negativity  $E_N$  and entanglement indicator  $I_{\text{ent}}$  is derived for pure states ( $I_S = 1/16$ ) assuming  $I_{\text{ent}} > 0$ :

$$E_N = \ln(2\sqrt{I_{\text{ent}}} + \sqrt{1 + 4I_{\text{ent}}}). \quad (23)$$

As we look for a relation among the local invariants  $I_{\text{ncl}}^{(1)}$  and  $I_{\text{ncl}}^{(2)}$  and the entanglement indicator  $I_{\text{ent}}$  (see Fig. 1), we eliminate the invariants  $I_3 = I_{S3}$  from Eqs. (13) and (19) by their comparing. This leaves us with the relation:

$$I_{\text{ncl}}^{(1)} + I_{\text{ncl}}^{(2)} + 2I_{\text{ent}} = \frac{1}{2}\Delta_S - \Delta - 2I_S - \frac{1}{8}. \quad (24)$$

TABLE II. Regions of different entanglement and local nonclassicalities observed in the figures of Secs. III–VI.

case/region	Entanglement	Nonclassicality of one mode	Nonclassicality of another mode	Figures
I	Yes	Yes	Yes	6, 10
II	Yes	Yes	No	6(b)
III	Yes	No	No	6, 10
IV	No	Yes	Yes	6, 10
V	No	Yes	No	6(b)
VI	No	No	No	6, 10

As only the global invariants occur at the r.h.s. of Eq. (24), the relation  $I_{\text{ncl}}^{(1)} + I_{\text{ncl}}^{(2)} + 2I_{\text{ent}}$  is invariant under any global linear unitary transformation.

Equation (24) can be transformed into the central result of our paper, if we define a new quantity  $I_{\text{ncl}}$ , which is a global nonclassicality invariant:

$$I_{\text{ncl}} = I_{\text{ncl}}^{(1)} + I_{\text{ncl}}^{(2)} + 2I_{\text{ent}}, \quad (25)$$

In the derivation of this equation, it is useful to recall the property that the local determinants for the normally-ordered CF,  $I_3$ , and the symmetrically-ordered CF,  $I_{S3}$ , are equal  $I_3 = I_{S3}$ , and given by Eqs. (14) and (18). Thus, we have

$$\begin{aligned}
I_{\text{ncl}} &= I_{\text{ncl}}^{(1)} + I_{\text{ncl}}^{(2)} + 2I_{\text{ent}} \\
&= -I_1 - I_2 + \frac{1}{2}(I_{S1} + I_{S2} - 2I_{S3}) - 2I_S - \frac{1}{8} \\
&= -I_1 - I_2 - 2I_{S3} + \frac{1}{2}(I_{S1} + I_{S2} + 2I_{S3}) - 2I_S - \frac{1}{8} \\
&= -\Delta + \frac{1}{2}\Delta_S - 2I_S - \frac{1}{8}.
\end{aligned} \quad (26)$$

We note that an invariant based on the second-order intensity moments and, as such, describing intensity auto- and cross-correlations has been suggested in Ref. [49] for two-mode fields with specific mode correlations and unitary transformations. Later, this invariant was experimentally analyzed in Ref. [50]. Here, we describe the propagation of fields through the beam splitter (see Fig. 1) described by the real transmissivity  $T$  and the phase  $\phi$  through the unitary transformation characterized by the matrix  $\mathbf{U}$ ,

$$\mathbf{U} = \begin{pmatrix} \sqrt{T} & 0 & -\sqrt{R}e^{i\phi} & 0 \\ 0 & \sqrt{T} & 0 & -\sqrt{R}e^{-i\phi} \\ \sqrt{R}e^{-i\phi} & 0 & \sqrt{T} & 0 \\ 0 & \sqrt{R}e^{i\phi} & 0 & \sqrt{T} \end{pmatrix}; \quad (27)$$

$R = 1 - T$  is the reflectivity of the beam splitter. The covariance matrix  $\mathbf{A}^{\text{out}}$  at the output of the beam splitter is obtained as  $\mathbf{A}^{\text{out}} = \mathbf{U}^\dagger \mathbf{A} \mathbf{U}$ .

Equation (25) means that the local nonclassicality invariants  $I_{\text{ncl}}^{(1)}$  and  $I_{\text{ncl}}^{(2)}$  together with the entanglement indicator  $I_{\text{ent}}$  form the global NI  $I_{\text{ncl}}$ . Any linear unitary transformation in general modifies both the local NIs  $I_{\text{ncl}}^{(1)}$  and  $I_{\text{ncl}}^{(2)}$  and the entanglement invariant  $I_{\text{ent}}$  only in such a way that it preserves the value of the global NI  $I_{\text{ncl}}$ . Whenever  $I_{\text{ncl}}$  is positive, the analyzed state is nonclassical due to the local nonclassicality of the reduced states or its entanglement. The negative values of the global NI  $I_{\text{ncl}}$  do not necessarily mean that a given state is classical, as we will see below.

In the next sections, we analyze the nonclassicality and entanglement of several kinds of important quantum states from the point of view of their transformation by a beam splitter. The division of the global NI into the EI and the local NIs is in the center of our attention. In general, six regions differing in the occurrence of entanglement and local nonclassicalities can be defined (see Table II). All these regions are found in the examples analyzed in the next sections, as indicated in Table II.

### III. TWIN BEAM

These beams are generated by parametric down-conversion from the vacuum into which photon pairs are ideally emitted. For this reason, only the terms  $B_1$ ,  $B_2$ , and  $D_{12}$  in the normal characteristic function  $C_{\mathcal{N}}$  are nonzero. The evolution matrices  $\mathbf{U}$  and  $\mathbf{V}$  in Eq. (6) have the following nonzero elements:

$$\begin{aligned}
U_{11}(t) &= U_{22}(t) = \cosh(gt), \\
V_{12}(t) &= V_{21}(t) = i \exp(i\theta) \sinh(gt).
\end{aligned} \quad (28)$$

The coefficients  $B_1$  and  $B_2$  can be expressed as  $B_1 = B_p + B_s$  and  $B_2 = B_p + B_i$ , where  $B_p = \sinh^2(g_{12}t)$  gives the mean number of generated photon pairs and  $B_s = \langle \hat{F}_1^\dagger \hat{F}_1 \rangle$  ( $B_i = \langle \hat{F}_2^\dagger \hat{F}_2 \rangle$ ) denotes the mean number of signal (idler) noise photons coming from the reservoir (see Fig. 2). On the other hand, the parameter  $D_{12}$  characterizing mutual correlations depends only on the mean num-

ber  $B_p$  of photon pairs as  $D_{12} = i\sqrt{B_p(B_p + 1)}$  ( $\theta = 0$  is assumed without the loss of generality).

The general formulas for the local NIs  $I_{\text{ncl}}^{(j)}$ , entanglement invariant  $I_{\text{ent}}$ , and the global NI  $I_{\text{ncl}}$  attain the following forms for twin beams:

$$\begin{aligned} I_{\text{ncl}}^{(1)} &= 4TR(B_p^2 + B_p) - [B_p + TB_s + RB_i]^2, \\ I_{\text{ncl}}^{(2)} &= 4TR(B_p^2 + B_p) - [B_p + TB_i + RB_s]^2, \\ I_{\text{ent}} &= -[(B_s + B_i)^2 - (T - R)^2](B_p^2 + B_p) \\ &\quad - 2B_p B_s B_i (B_s + B_i) - (B_s^2 + B_s)(B_i^2 + B_i) \\ &\quad - TR(B_s + B_i)^2, \end{aligned} \quad (29)$$

$$\begin{aligned} I_{\text{ncl}} &= 2B_p - (B_s + B_i)^2[2(B_p^2 + B_p) + 1] \\ &\quad - 2B_p(1 + 2B_s B_i)(B_s + B_i) \\ &\quad - 2B_s B_i(B_s + B_i + B_s B_i). \end{aligned} \quad (30)$$

We first discuss the behavior of noiseless twin beams for which  $B_s = B_i = 0$ . In this case, the global NI  $I_{\text{ncl}}$  equals  $2B_p$  and

$$\begin{aligned} I_{\text{ncl}}^{(j)} &= 4TR(B_p^2 + B_p) - B_p^2, \quad j = 1, 2, \\ I_{\text{ent}} &= (T - R)^2(B_p^2 + B_p). \end{aligned} \quad (31)$$

As suggested by the formula in Eq. (31), the local NIs  $I_{\text{ncl}}^{(j)}$  can be decomposed into two terms. The negative term reflects classical thermal statistics of photon pairs in a twin beam with its photon bunching effect and as such suppresses the nonclassical behavior of the twin beam. On the other hand, the positive term refers to squeezing appearing at the individual output ports of the beam splitter. The squeezing effect originates in pairing of photons in individual output ports caused by “sticking of two photons from a pair together” (photon bunching) at the beam splitter [5]. Photon pairs with both photons in one output port contribute to the local nonclassicality of the field in this port. On the other hand, when two photons from one photon-pair occur in different output ports, they contribute to the entanglement. “A given individual photon pair” is, thus, responsible either for the local nonclassicality in one of the output ports or for their entanglement. Never for both. Propagation through the beam splitter can, thus, be viewed as the process of breaking photon pairs (antibunching) arriving at the same input port and gluing (bunching) of photons from a given pair coming from different input ports. Whereas the first process disturbs local squeezing and supports entanglement, the second process strengthens squeezing at the expense of entanglement. The global NI  $I_{\text{ncl}}$  is equal twice the number  $B_p$  of photon pairs and, as such, indicates an appropriate choice of this nonclassicality resource quantifier.

Detailed analysis of the formulas in Eq. (31) shows that the local marginal states are nonclassical only if the transmissivity  $T$  lies in certain interval around  $\frac{1}{2}$ :

$$T \in \left( \frac{1}{2} - \frac{1}{2\sqrt{B_p + 1}}, \frac{1}{2} + \frac{1}{2\sqrt{B_p + 1}} \right). \quad (32)$$

It holds that the larger is the mean photon-pair number  $B_p$ , the narrower is the interval. The optimal transmissivity  $T$  maximizing the local NIs  $I_{\text{ncl}}^{(j)}$  equals  $\frac{1}{2}$ . In this case, the entanglement of the incident twin beam is completely and equally transferred into the local nonclassicalities of the two output modes. On the other hand, the twin beam loses its entanglement only when  $T = \frac{1}{2}$ . In this case, all the incident photon pairs stick together (bunch) at the beam splitter suppressing completely their entanglement. Hand in hand, the local NIs  $I_{\text{ncl}}^{(1)} = I_{\text{ncl}}^{(2)}$  attain their maximal values. This can be interpreted such that the initial entanglement is transferred into the squeezing of the marginal output fields [51]. These effects are shown in Figs. 4(a) and 5(a) for the dependencies of the local NI  $I_{\text{ncl}}^{(1)}$  and EI  $I_{\text{ent}}$  on the transmissivity  $T$  and mean photon-pair number  $B_p$ . The commonly used the Lee nonclassicality depth  $\tau_1$  and the logarithmic negativity  $E_N$  are shown for comparison in Figs. 4(b) and 5(b). We note, that whereas the values of the Lee nonclassicality depth  $\tau_1$  cannot exceed  $\frac{1}{2}$ , the values of the local NI  $I_{\text{ncl}}^{(1)}$  can be arbitrarily large depending on the intensity of the twin beam.

Now we consider general noisy twin beams. It has been shown in Ref. [36] that whenever the overall noise  $B_s + B_i$  exceeds one, the twin beam is unentangled and, thus, it cannot generate any nonclassical feature. Even if  $B_s + B_i < 1$ , the mean photon-pair number  $B_p$  has to be sufficiently large, as given by

$$B_p > \frac{B_s B_i}{1 - (B_s + B_i)}. \quad (33)$$

Then, the incident noisy twin beam is entangled and is capable to provide its entanglement and local nonclassicality after the beam splitter. However, the general analysis of Eqs. (29) and (30) leads to the conclusion that the noise only degrades the non-classical behavior independently whether it is manifested by local nonclassicality or entanglement. The stronger the noise, the weaker the non-classical features.

To provide a deeper insight into the role of noise, we analyze two special cases: in the first one, the noise is equally divided into both modes of the incident twin beam; while noise occurs only in one mode of the incident twin beam in the second case.

When noise occurs in both modes of the incident twin beam ( $B_n \equiv B_s = B_i$ ), the globally nonclassical output states can be divided into three groups. They are displayed in the “phase diagram” in Fig. 6. In this diagram, the surfaces  $I_{\text{ncl}}^{(1)}(B_n, B_p, T) = 0$  and  $I_{\text{ent}}(B_n, B_p, T) = 0$  are shown. They identify four different regions belonging to different groups of states (see Table II for details). The states exhibiting both entanglement and local nonclassicality occur in region I. In region III, the states are entangled but locally classical. The locally nonclassical and unentangled states are found in region IV. In region VI, the unentangled and locally classical states exist.



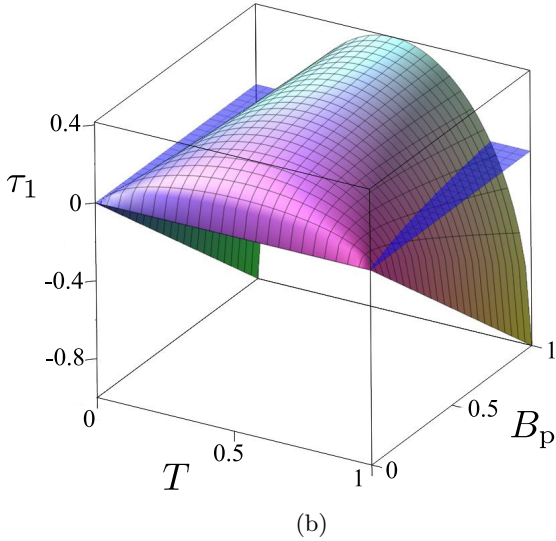
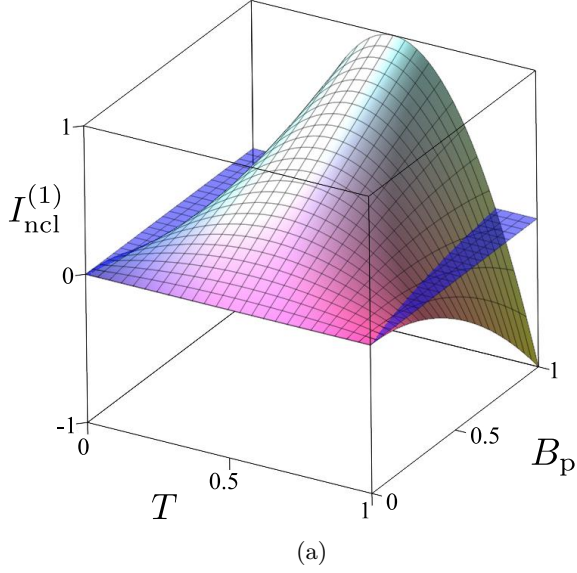


FIG. 4. (Color online) (a) Local nonclassicality invariant  $I_{\text{ncl}}^{(1)}$  and (b) continuous Lee nonclassicality depth  $\tau_1$  (including negative values) at the output port 1 of the beam splitter as a function of the mean photon-pair number  $B_p$  and the beam-splitter transmissivity  $T$  for pure twin beam states. In panel (a) and (b), the blue dark grey plain surface at  $I_{\text{ncl}}^{(1)} = 0$  and  $\tau_1 = 0$  shows the boundary between the classical and nonclassical domains.

The presence of noise in only one mode of the incident twin beam ( $B_s = 0$ ,  $B_i \equiv B_n \neq 0$ ) leads to asymmetry between the output modes. This is shown in Fig. 7, where the surfaces  $I_{\text{ncl}}^{(1)}(B_n, B_p, T) = 0$  and  $I_{\text{ncl}}^{(2)}(B_n, B_p, T) = 0$  behave differently. The symmetry, with respect to the plane for  $T = \frac{1}{2}$ , which is clearly visible in Fig. 6, does not exist in Fig. 7. As a consequence, two additional groups of states are found in the diagram. In region V, there are unentangled states with

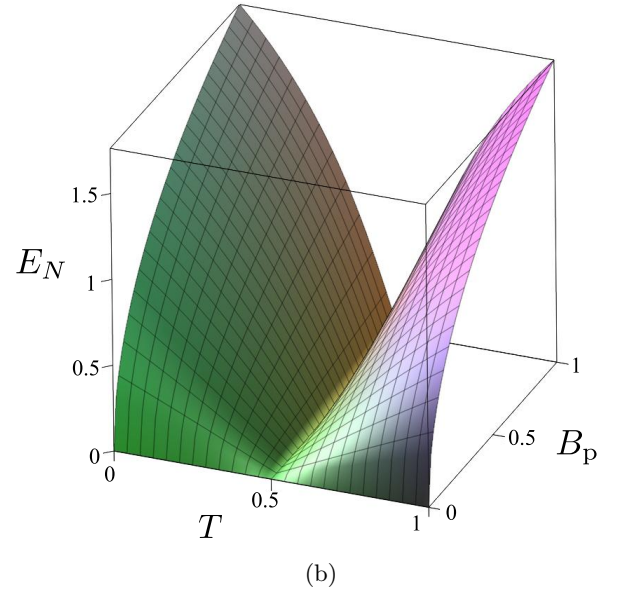
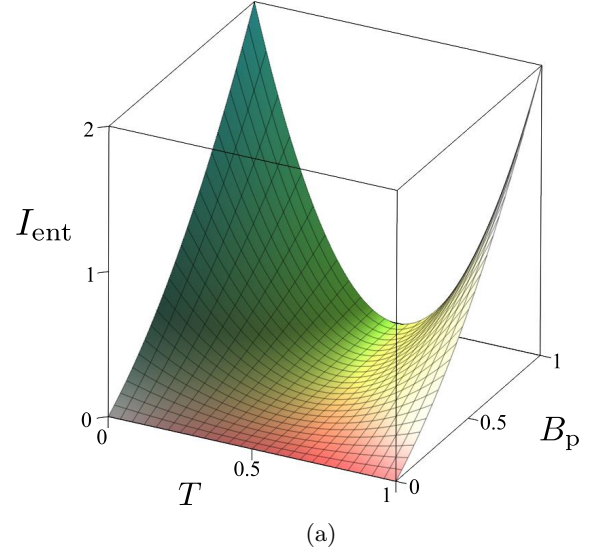


FIG. 5. (Color online) (a) Entanglement invariant  $E_I$  and (b) logarithmic negativity  $E_N$  after the beam splitter transformation considered as functions of the mean photon-pair number  $B_p$  and the beam-splitter transmissivity  $T$  for pure twin beams states.

only one marginal field exhibiting local nonclassicality. The entangled states with only one locally nonclassical field are found in region II. In detail, mode 1 (2) is locally nonclassical for  $T < \frac{1}{2}$  ( $T > \frac{1}{2}$ ). We note that the EI  $I_{\text{ent}}$  is not sensitive to the noise asymmetry, as shown by the surface  $I_{\text{ent}}(B_n, B_p, T) = 0$  in Fig. 7. It is worth noting that positive values of the GNI  $I_{\text{ncl}}$  are exhibited when either entanglement or local nonclassicality or even both are found. The negative values of the global NI  $I_{\text{ncl}}$  do not necessarily mean classicality. The state with the negative GNI  $I_{\text{ncl}}$  can still be globally nonclassical due to



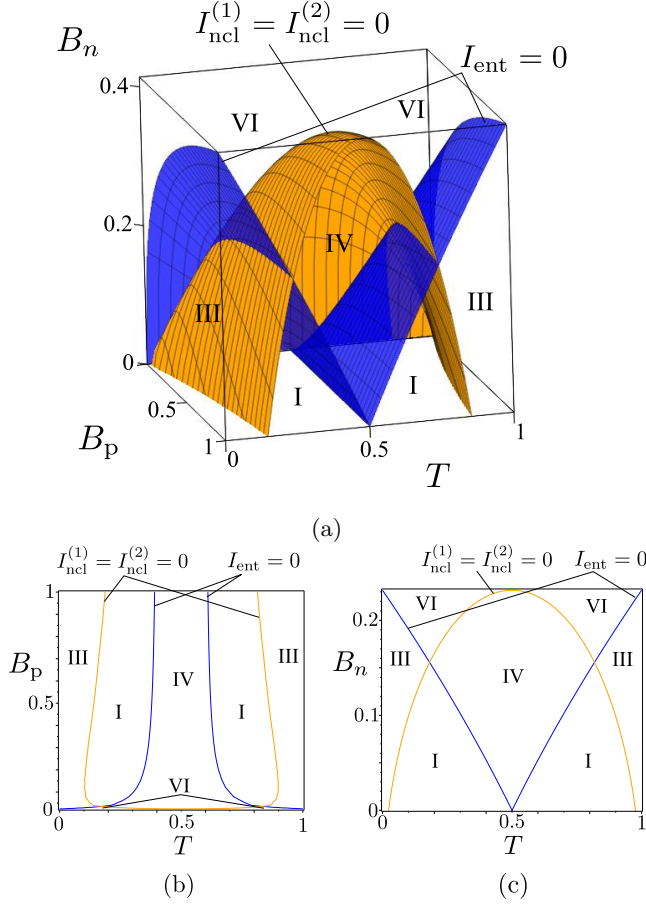


FIG. 6. (Color online) Diagram (a) shows the nonclassicality and entanglement invariants for the twin beams states occurring at the output ports of a beam splitter depending on the mean noise photon number  $B_n$ , mean photon-pair number  $B_p$ , and transmissivity  $T$  according to Eq. (29) for  $B_n \equiv B_s = B_i$ . The surfaces are plotted at  $I_{\text{ncl}}^{(1)}(B_n, B_p, T) = 0$  [orange light gray surface],  $I_{\text{ncl}}^{(2)}(B_n, B_p, T) = 0$  [orange light gray] and  $E_I(B_n, B_p, T) = 0$  [blue dark surface] indicating six different regions specified in the text and Tab. II. Diagrams (b) and (c) show the perpendicular cross-sections of diagram (a) taken at chosen values of  $B_n = 0.1$  and  $B_p = 0.1$ , respectively.

either its entanglement or local nonclassicality, but not both. The diagram in Fig. 6(a) can serve as an example. The surface  $I_{\text{ncl}}(B_n, B_p, T) = 0$  lies naturally in between the surfaces  $I_{\text{ncl}}^{(1)}(B_n, B_p, T) = 0$ , and  $I_{\text{ent}}(B_n, B_p, T) = 0$  and its position identifies the globally nonclassical states with  $I_{\text{ncl}} < 0$ .

#### IV. SQUEEZED VACUUM STATE WITH NOISE

Here, we consider a squeezed vacuum state [5] mixed with the noise incident on one input port of the beam splitter, whereas the second input port is left in the vacuum state. In this case, the nonzero elements of evolu-

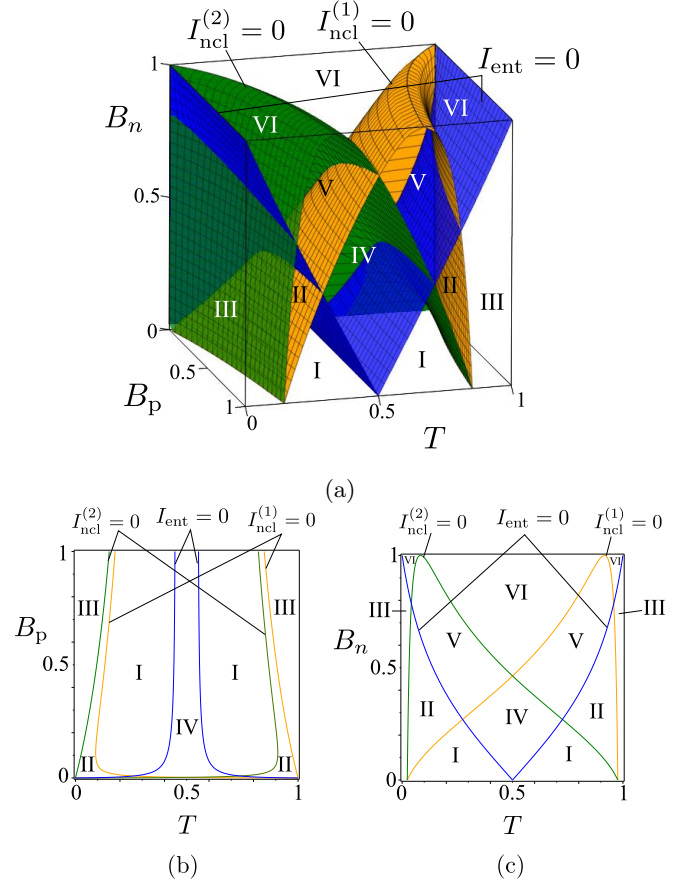


FIG. 7. (Color online) Diagram (a) shows the nonclassicality and entanglement invariants for the twin beams states occurring at the output ports of a beam splitter depending on the mean noise photon number  $B_n$ , mean photon-pair number  $B_p$ , and transmissivity  $T$  according to Eq. (29) for  $B_s = 0$  and  $B_n = B_i$ . The surfaces are plotted at  $I_{\text{ncl}}^{(1)}(B_n, B_p, T) = 0$  [orange light gray surface],  $I_{\text{ncl}}^{(2)}(B_n, B_p, T) = 0$  [green dark gray surfaces] and  $E_I(B_n, B_p, T) = 0$  [blue dark surface] indicating six different regions specified in the text and Tab. II. Diagrams (b) and (c) show the perpendicular cross-sections of diagram (a) taken at fixed values of  $B_n = 0.1$  and  $B_p = 0.1$ , respectively. These cross-sections are analogous to those in Figs. 6(b) and 6(c).

tion matrices  $\mathbf{U}$  and  $\mathbf{V}$  in Eq. (6) are given as ( $\theta = 0$  is assumed):

$$\begin{aligned} U_{11}(t) &= \cosh(gt), & U_{22}(t) &= 1, \\ V_{11}(t) &= i \exp(i\theta) \sinh(gt). \end{aligned} \quad (34)$$

The non-zero parameters of the normal characteristic function  $\mathcal{N}$  in Eq. (10) are  $B_1$  and  $C_1$  as given by:  $B_1 = \tilde{B}_p^{\text{sq}} + B_s$  and  $C_1 = i\sqrt{\tilde{B}_p^{\text{sq}}(\tilde{B}_p^{\text{sq}} + 1)}$ . The symbol  $\tilde{B}_p^{\text{sq}}$  denotes the mean number of squeezed photons and the symbol  $B_s$  stands for the mean number of the signal noise photons (see also Fig. 2). The local NIs  $I_{\text{ncl}}^{(j)}$  and EI  $I_{\text{ent}}$  are easily expressed in terms of the global NI

$I_{\text{ncl}}$  as follows

$$I_{\text{ncl}}^{(1)} = T^2 I_{\text{ncl}}, \quad I_{\text{ncl}}^{(2)} = R^2 I_{\text{ncl}}, \quad I_{\text{ent}} = TRI_{\text{ncl}},$$

$$I_{\text{ncl}} = \tilde{B}_p^{\text{sq}}(1 - 2B_s) - B_s^2. \quad (35)$$

As the local NIs  $I_{\text{ncl}}^{(1)}$  and  $I_{\text{ncl}}^{(2)}$ , as well as the EI  $I_{\text{ent}}$  are linearly proportional to the global NI  $I_{\text{ncl}}$ , the global nonclassicality of the output states immediately guarantees both local nonclassicalities and entanglement. This occurs only for the positive values of the global NI  $I_{\text{ncl}}$ . According to Eq. (35),  $I_{\text{ncl}} > 0$  provided that the mean noise photon number  $B_s$  in the signal mode is sufficiently small:

$$B_s < \sqrt{\tilde{B}_p^{\text{sq}}(\tilde{B}_p^{\text{sq}} + 1)} - \tilde{B}_p^{\text{sq}}. \quad (36)$$

Following Eq. (35), the mean noise photon number  $B_s$  in the signal mode has to be smaller than 1. Also, the more intense is the squeezed state, the smaller is the number  $B_s$  of accepted noise photons. We note that the condition, given in Eq. (35), can immediately be revealed when the global Lee nonclassicality depth  $\tau$  is analyzed. As an illustration, the dependencies of the local NIs  $I_{\text{ncl}}^{(1)}$  and  $I_{\text{ncl}}^{(2)}$  and the EI  $I_{\text{ent}}$  on the beam-splitter transmissivity  $T$  are plotted in Fig. 8 for the incident noiseless squeezed states. The greatest values of EI  $I_{\text{ent}}$  are reached for the balanced beam splitter ( $T = \frac{1}{2}$ ). However, some incident photon pairs are not broken (i.e., split) by the beam splitter and give raise to nonzero local nonclassicalities  $I_{\text{ncl}}^{(1)}$  and  $I_{\text{ncl}}^{(2)}$  even in this case.

The strength of squeezing in a given mode is commonly characterized by a principal squeeze variance  $\lambda$  [52], which is here given by

$$\lambda_j = 1/2 + B_j - |C_j|. \quad (37)$$

When a given output mode  $j = 1, 2$  is locally nonclassical, it is also squeezed, which corresponds to  $\lambda_j < \frac{1}{2}$ . According to the relation between the local NI  $I_{\text{ncl}}^{(j)}$  and the principal squeeze variance  $\lambda_j$  derived by combining Eqs. (16) and (37),

$$I_{\text{ncl}}^{(j)} = \left(\frac{1}{2} - \lambda_j\right)(2B_j + \frac{1}{2} - \lambda_j), \quad (38)$$

the smaller is the value of the principal squeeze variance  $\lambda_j$  below  $\frac{1}{2}$ , the greater is the value of the local NI  $I_{\text{ncl}}^{(j)}$ .

## V. TWO SQUEEZED VACUA

Two independent squeezed states are generated by the Hamiltonian given in Eq. (2) provided that the process of parametric down-conversion does not occur in the non-linear medium ( $g_{12} = 0$ ). The solution of the evolution governed by the Hamiltonian (2) gives us the following nonzero elements of the evolution matrices  $\mathbf{U}$  and  $\mathbf{V}$ :

$$U_{11} = \cosh(2g_{11}t), \quad V_{11} = i \exp(i\kappa_1) \sinh(2g_{11}t),$$

$$U_{22} = \cosh(2g_{22}t), \quad V_{22} = i \exp(i\kappa_2) \sinh(2g_{22}t), \quad (39)$$

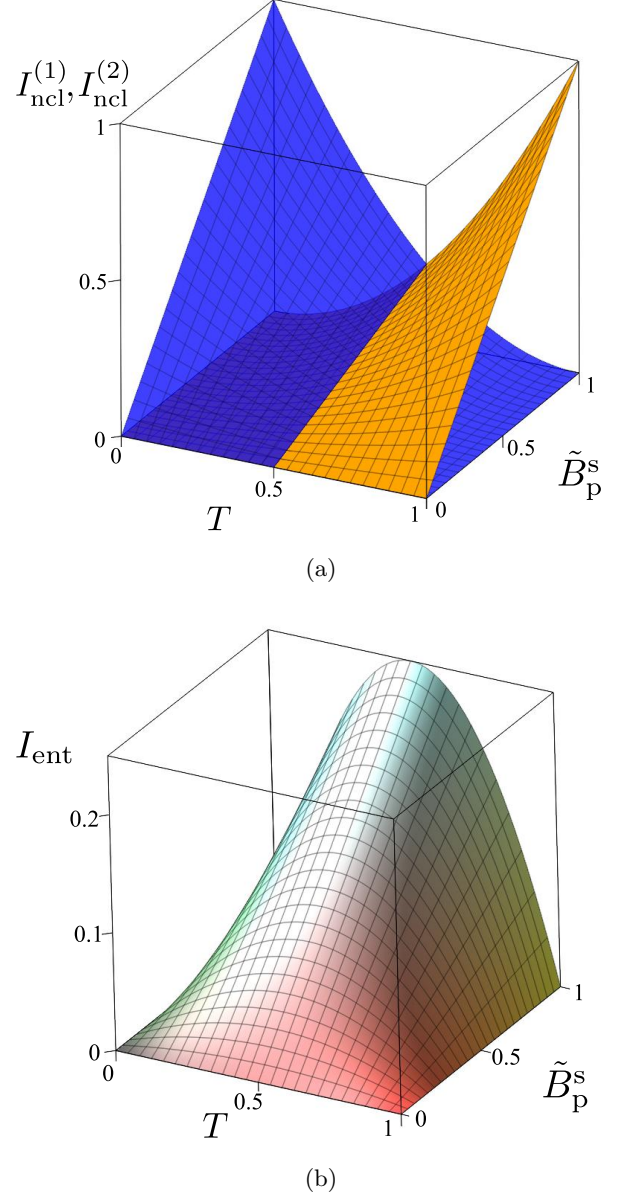


FIG. 8. (Color online) Invariant nonclassicality parameters: (a) the local nonclassicality invariants  $I_{\text{ncl}}^{(1)}$  (orange light gray surface) and  $I_{\text{ncl}}^{(2)}$  (blue dark gray surface), and (b) the entanglement invariant  $I_{\text{ent}}$  versus the mean number  $\tilde{B}_p^s$  of squeezed photons and the beam-splitter transmissivity  $T$  according to Eq. (35) assuming  $B_s = 0$ .

where  $\kappa_1$  and  $\kappa_2$  are arbitrary phases. The nonzero coefficients of the incident covariance matrix  $\mathbf{A}_{\mathcal{N}}$  are given as  $B_{1,2} = \tilde{B}_p^{s,i} + B_{s,i}$  and  $C_{1,2} = \exp(i\theta_{1,2})\sqrt{\tilde{B}_p^{s,i}(\tilde{B}_p^{s,i} + 1)}$ ,  $\theta_j = \kappa_j + \pi/2$  for  $j = 1, 2$ , where  $\tilde{B}_p^s$  ( $\tilde{B}_p^i$ ) stands for the mean number of squeezed photons in the signal (idler) mode, whereas the corresponding mean signal (idler) noise photon number is denoted as  $B_s$  ( $B_i$ ).

After the beam splitter, the local NIs  $I_{\text{ncl}}^{(j)}$ , EI  $I_{\text{ent}}$  and

global NI  $I_{\text{ncl}}$  acquire the form:

$$\begin{aligned}
I_{\text{ncl}}^{(1)} &= T^2 \tilde{B}_p^s (\tilde{B}_p^s + 1) + R^2 \tilde{B}_p^i (\tilde{B}_p^i + 1) + TR \bar{D}'_{12} \cos(\theta_1 - \theta_2) - [T \tilde{B}_p^s + R \tilde{B}_p^i + T B_s + R B_i]^2, \\
I_{\text{ncl}} &= B_1 + B_2 - 2B_s B_i \left[ 2B_1(1 + \tilde{B}_p^i) + 2\tilde{B}_p^i(1 + B_1) + B_i(1 + 2B_1) + B_s(1 + 2B_2) \right] - 2(B_s B_1 + B_i B_2) - (B_s + B_i)^2, \\
I_{\text{ent}} &= TR \left[ -\bar{D}'_{12} \cos(\theta_1 - \theta_2) + (\tilde{B}_p^s + \tilde{B}_p^i + 2\tilde{B}_p^s \tilde{B}_p^i) - (B_s + B_i)^2 - 2(\tilde{B}_p^s - \tilde{B}_p^i)(B_s - B_i) \right] \\
&\quad + B_s B_i \left[ 2\tilde{B}_p^s(1 + B_i) + 2\tilde{B}_p^i(1 + B_s) + 4\tilde{B}_p^s \tilde{B}_p^i + (1 + B_s)(1 + B_i) \right],
\end{aligned} \tag{40}$$

where  $\bar{D}'_{12} = 2\sqrt{\tilde{B}_p^s(\tilde{B}_p^s + 1)\tilde{B}_p^i(\tilde{B}_p^i + 1)}$ ,  $B_1 = \tilde{B}_p^s + B_s$ ,  $B_2 = \tilde{B}_p^i + B_i$ , and, for simplicity, we assumed  $\phi = 0$  in Eq. (27). The formula for  $I_{\text{ncl}}^{(2)}$  is obtained from that for  $I_{\text{ncl}}^{(1)}$  in Eq. (40) with the substitution  $s \leftrightarrow i$ .

The global NI  $I_{\text{ncl}}$  does not depend on the relative phase  $\Delta\theta = \theta_1 - \theta_2$  of two incident squeezed states, while the local NIs  $I_{\text{ncl}}^{(j)}$  and EI  $I_{\text{ent}}$  change with the relative phase  $\Delta\theta$ . The case of two equally intense incident noiseless squeezed states, as graphically analyzed in Fig. 9, shows that the phase difference  $\Delta\theta$  plays a crucial role in distributing the nonclassicality between the output entanglement and local nonclassicalities. If the phases  $\theta_1$  and  $\theta_2$  are equal, the incident photon pairs stick (bunch) ideally together due to the interference at the beam splitter and the incident locally-nonclassical squeezed states are moved into the output ports. No photon pair is broken and so no entanglement is observed. On the other hand, if  $\Delta\theta = \pi$ , then some incident photon pairs are broken and, thus, the output squeezing (as well as local nonclassicalities) is weaker. The broken photon pairs give rise to the entanglement. The value of EI  $I_{\text{ent}}$  is maximal for the transmissivity  $T = \frac{1}{2}$ . In this case, all the photon pairs are broken, their signal and idler photons occur in different output ports and, as a consequence, the ideal conditions for entanglement generation are met. Hand in hand, the vanishing local NIs  $I_{\text{ncl}}^{(j)}$  are found (see Fig. 9).

It is remarkable that the global NI  $I_{\text{ncl}}$  for the equally intense noiseless squeezed states is given formally by the same formula as that valid for the noiseless twin beams considering the mean photon-pair number  $B_p$  instead of  $\tilde{B}_p^s = \tilde{B}_p^i \equiv \tilde{B}_p$ . However, the incident twin beam serves as a source of locally-nonclassical (squeezed) states, whereas the incident squeezed states provide entangled states at the output of the beam splitter. The comparison of graphs in Figs. 4(a) and 5(a) with those in Figs. 10(a) and 10(b) reveals that the incident noiseless squeezed states generate entangled states for an arbitrary value of the transmissivity  $T$ , but the incident noiseless twin beams are capable of the generation of the output squeezed states only in a certain interval of the transmis-

sivity  $T$  depending on the intensity.

Similarly as for the twin beams, the noise diminishes the global NI  $I_{\text{ncl}}$  [see the formula for  $I_{\text{ncl}}$  in Eq. (40)]. Considering the incident states with  $\tilde{B}_p^s = \tilde{B}_p^i$  and  $B_s = B_i$ , the presence of noise leads to the occurrence of the three different types of globally nonclassical states already discussed in the connection with the noisy twin beams with symmetric noise. Regions corresponding to different types of the output states are shown in the diagram in Fig. 11(a) that can be compared with that of Fig. 6(a).

## VI. TWIN BEAM MIXED WITH SQUEEZED STATES

Finally, we analyze an interplay of noiseless twin beams and equally populated noiseless squeezed states ( $\Delta\theta = 0$ ) in forming the output state at the beam splitter with phase  $\phi$ . Such state is generated by the Hamiltonian (2) assuming  $g_{11} = g_{22} = g$  and described by the following elements of the evolution matrices  $\mathbf{U}$  and  $\mathbf{V}$ :

$$\begin{aligned}
U_{11} &= U_{22} = \cosh(g_{12}t) \cosh(2gt), \\
V_{11} &= V_{22} = i \cosh(g_{12}t) \sinh(2gt), \\
U_{12} &= U_{21} = \sinh(g_{12}t) \sinh(2gt), \\
V_{12} &= V_{21} = i \sinh(g_{12}t) \cosh(2gt).
\end{aligned} \tag{41}$$

Introducing the mean photon-pair number  $B_p$  as  $B_p = \sinh^2(g_{12}t)$  and mean number  $\tilde{B}_p$  of squeezed photons per mode,  $\tilde{B}_p = \sinh^2(2gt)$ , the coefficients of the covariance matrix  $\mathbf{A}_{\mathcal{N}}$  are found in the form:

$$\begin{aligned}
B_1 &= B_2 = B_p + \tilde{B}_p + 2B_p \tilde{B}_p, \\
C_1 &= C_2 = i\sqrt{\tilde{B}_p(\tilde{B}_p + 1)}(2B_p + 1), \\
D_{12} &= i\sqrt{B_p(B_p + 1)}(2\tilde{B}_p + 1), \\
\bar{D}_{12} &= -2\sqrt{B_p(B_p + 1)\tilde{B}_p(\tilde{B}_p + 1)}.
\end{aligned} \tag{42}$$

The local NIs  $I_{\text{ncl}}^{(j)}$ , EI  $I_{\text{ent}}$ , and global NI  $I_{\text{ncl}}$  are then

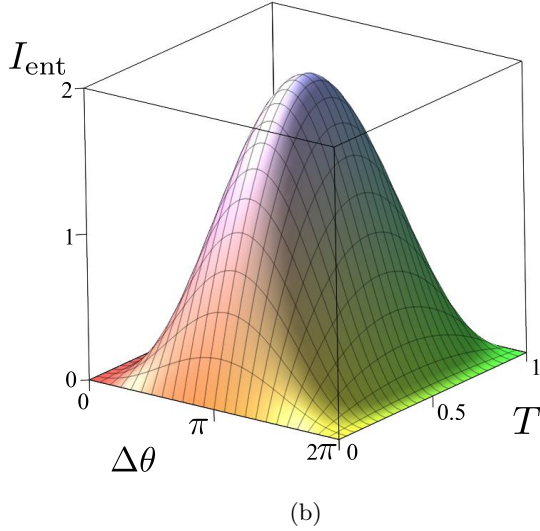
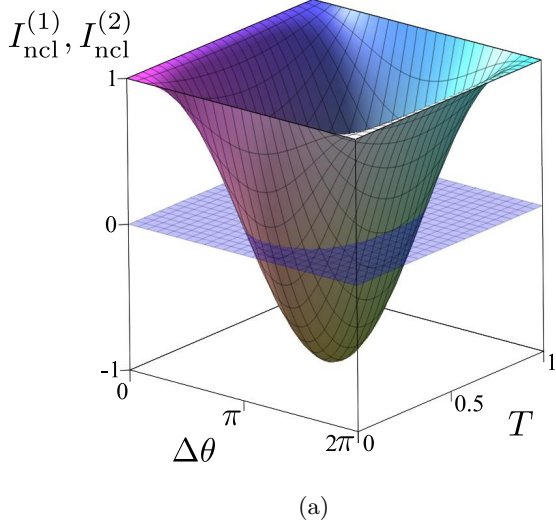


FIG. 9. (Color online) (a) Local nonclassicality invariants  $I_{\text{ncl}}^{(1)} = I_{\text{ncl}}^{(2)}$  and (b) entanglement invariant  $I_{\text{ent}}$  versus the phase difference  $\Delta\theta$  and beam-splitter transmissivity  $T$  for two noiseless squeezed states according to Eq. (40);  $\tilde{B}_p^s = \tilde{B}_p^i = 1$ . In panel (a), the blue surface at  $I_{\text{ncl}}^{(1)} = I_{\text{ncl}}^{(2)} = 0$  shows the boundary between classical and nonclassical states.

derived as follows:

$$\begin{aligned}
 I_{\text{ncl}}^{(1,2)} &= [1 - 4TR \sin^2(\phi)] \tilde{B}_p (\tilde{B}_p + 1) + 4TR B_p (B_p + 1) \\
 &\quad - (\tilde{B}_p - B_p)^2 \pm K, \\
 K &= 4\sqrt{TR} \cos(\phi) \sqrt{B_p (B_p + 1) \tilde{B}_p (\tilde{B}_p + 1)}, \\
 I_{\text{ent}} &= (T - R)^2 B_p (B_p + 1) + 4TR \sin^2(\phi) \tilde{B}_p (\tilde{B}_p + 1), \\
 I_{\text{ncl}} &= 2(B_p + \tilde{B}_p + 2B_p \tilde{B}_p). \tag{43}
 \end{aligned}$$

The formula for the global NI  $I_{\text{ncl}}$ , given in Eq. (43), shows that both parametric down-conversion and second subharmonic generation contribute to the global NI mak-

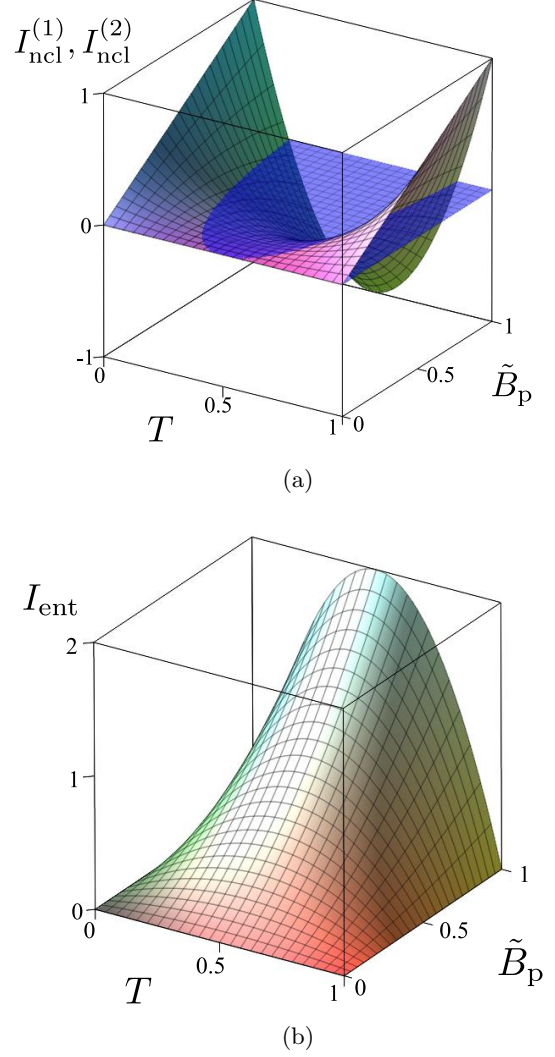


FIG. 10. (Color online) (a) Local nonclassicality invariant  $I_{\text{ncl}}^{(1)}$  and (b) entanglement invariant  $I_{\text{ent}}$  versus the beam-splitter transmissivity  $T$  and mean number  $\tilde{B}_p$  of squeezed photons for two noiseless squeezed states according to Eq. (40);  $\tilde{B}_p \equiv \tilde{B}_p^s = \tilde{B}_p^i$ ;  $\Delta\theta = \pi$ . In panel (a) the blue surface at  $I_{\text{ncl}}^{(1)} = I_{\text{ncl}}^{(2)} = 0$  shows the boundary between classical and nonclassical states.

ing  $I_{\text{ncl}}$  always positive. Moreover, both processes enhance each other in producing larger values of the global NI. The greater is the mean photon-pair number  $B_p$  and also the greater is the mean number  $\tilde{B}_p$  of squeezed photons, the greater is the global NI  $I_{\text{ncl}}$  (see Fig. 12). Additionally, both LNI  $I_{\text{ncl}}^{(j)}$  and EI  $I_{\text{ent}}$  become dependent on the phase  $\phi$  of the beam splitter.

Provided that the phases of the incident squeezed states equal ( $\phi = n\pi$ ,  $n \in \mathbb{Z}$ ), photons in pairs stick together (bunch) completely when propagating through the beam splitter and so they cannot contribute to the entanglement in the output state. In this case, the en-



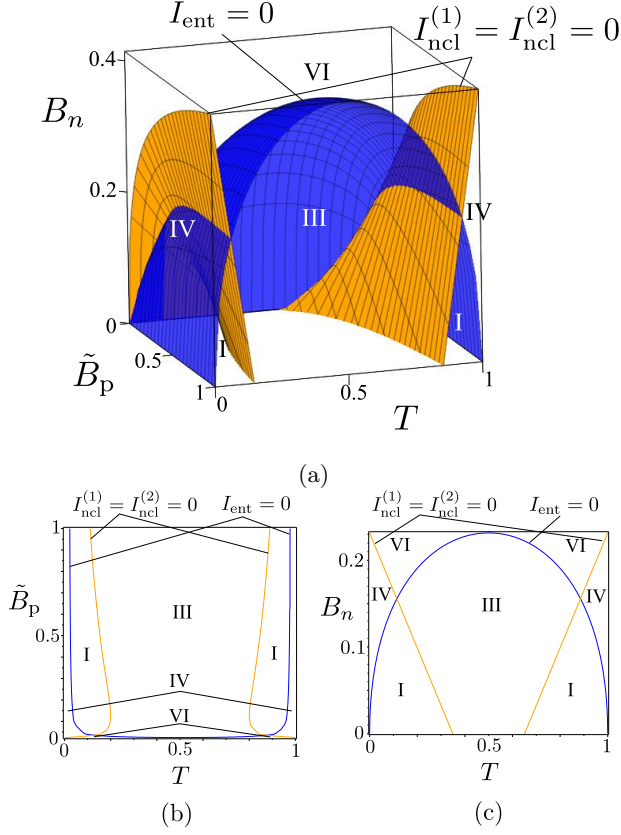


FIG. 11. (Color online) Diagram (a) shows the nonclassicality and entanglement invariants for the two squeezed vacua occurring at the output ports of the beam splitter versus the mean noise photon number  $B_n$ , mean number  $\tilde{B}_p$  of squeezed photons and transmissivity  $T$  assuming  $B_n \equiv B_s = B_i$  and  $\tilde{B}_p \equiv \tilde{B}_p^s = \tilde{B}_p^i$  and  $\Delta\theta = \pi$ . Surfaces at  $I_{\text{ncl}}^{(j)}(B_n, \tilde{B}_p, T) = 0$  ( $j = 1, 2$ ) (orange light gray) and  $I_{\text{ent}}(B_n, \tilde{B}_p, T) = 0$  (blue dark gray) are shown surrounding different regions specified in Tab. II. Diagrams (b) and (c) show the perpendicular cross-sections of diagram (a) taken at given values of  $B_n = 0.1$  and  $\tilde{B}_p = 0.1$ , respectively. These cross-sections can be compared with those in panels (b) and (c) in Figs. 6 and 7.

tanglement originates only in photon pairs of the incident twin beam. When  $T = 1/2$  all photons in pairs from the twin beam are glued and so the output state is separable. Contrary to this, the local NIs  $I_{\text{ncl}}^{(j)}$  depend on both mean photon-pair number  $B_p$  and mean number  $\tilde{B}_p$  of squeezed photons. The fields characterizing photon pairs in individual output ports and originating in the incident squeezed states and the incident twin beam interfere causing the asymmetry between the output ports. Depending on the parity of  $n$  one obtains the maximal local NI  $I_{\text{ncl}}^{(1)}$  ( $I_{\text{ncl}}^{(2)}$ ) if  $n = 2k$  ( $n = 2k+1$ ),  $k \in \mathbb{Z}$ . This asymmetry is the largest for  $T = 1/2$ . In this case, the bunched photon pairs are completely missing in one output port due to completely destructive interference. On the other hand, constructive interference provides the

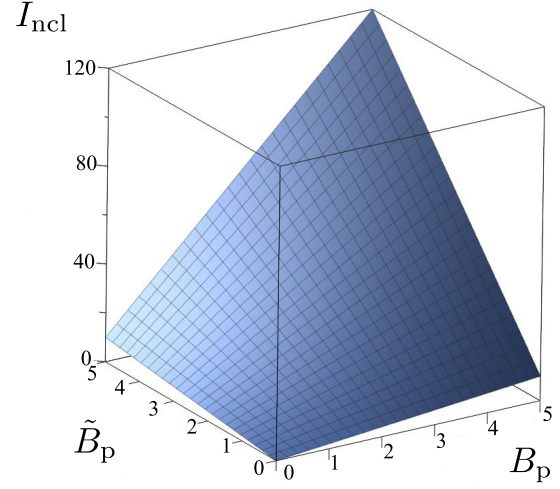


FIG. 12. (Color online) Global nonclassicality invariant  $I_{\text{ncl}}$  as a function of the mean photon-pair number  $B_p$  and mean number  $\tilde{B}_p$  of squeezed photons considering the noiseless twin beams and squeezed states.

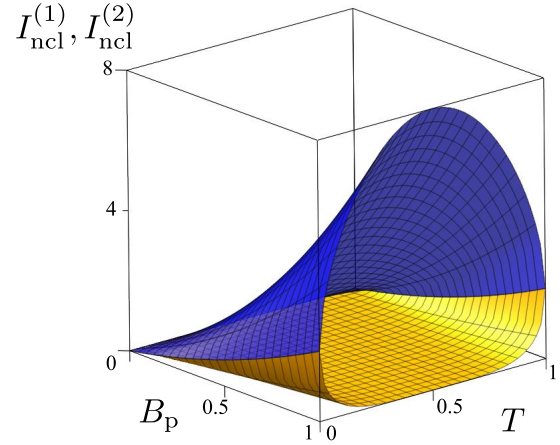


FIG. 13. (Color online) Local nonclassicality invariants  $I_{\text{ncl}}^{(1)}$  (blue dark upper surface) and  $I_{\text{ncl}}^{(2)}$  (orange light coloured lower surface) versus the beam-splitter transmissivity  $T$  and mean photon-pair number  $B_p$  assuming  $B_p = \tilde{B}_p$  appropriate for the noiseless twin beams and squeezed states according to Eq. (43) assuming  $\phi = 0$ .

greatest number of the bunched photon pairs in the other output port guaranteeing the largest attainable value of its local NI  $I_{\text{ncl}}^{(j)}$ . This behavior is quantified in the graph in Fig. 13.

If  $\phi = \frac{\pi}{2} + n\pi$ , the local NIs are equal ( $I_{\text{ncl}}^{(1)} = I_{\text{ncl}}^{(2)}$ ) and the state at the beam-splitter output ports acquires a symmetry. Under these phase relations, also the incident squeezed photon pairs contribute, together with the twin-beam photon pairs, to the entanglement. It is worth noting that for  $B_p = \tilde{B}_p$  all the state quantifiers are the same:  $I_{\text{ncl}}^{(1)} = I_{\text{ncl}}^{(2)} = I_{\text{ent}} = B_p(B_p + 1)$ .

## VII. CONCLUSIONS

Local and global invariants of the general two-mode Gaussian states have been used to construct a specific local nonclassicality quantifier and entanglement quantifier. These quantifiers applied, respectively, to the single-mode marginal states and the whole two-mode state add together to give a quantity that is invariant under global linear unitary transformations. This invariant then quantifies the nonclassicality resources of Gaussian states. Remarkably, this invariant is linearly proportional to the number of photon pairs in the noiseless Gaussian states. The general results have been used to study the beam-splitter transformations of fields composed of photon pairs and additional noisy photons. Twin beams, squeezed states as well as their combinations have been considered as important examples. The behavior of photon pairs at the beam splitter causing their breaking or gluing (i.e., antibunching or bunching) has been used to explain the flow of nonclassical resources between local nonclassicalities (implying squeezing) and entanglement. A complete transfer of the entanglement of incident twin beams into the squeezing of the output modes has been observed. Also the complete transfer of the incident squeezing into the entanglement of the output fields can be reached. The role of noise in the transfer of the nonclassicality invariant via the beam splitter has been elucidated on several examples.

## ACKNOWLEDGMENTS

The authors thank Jiří Svozilík and Anirban Pathak for discussions. This work was supported by the projects No. P205/12/0382 of the GA CR and No. LO1305 of the MSM CR. I.A. acknowledges the project IGA\_PrF\_2016\_002 of IGA UP Olomouc. A.M. acknowledges the support of a grant from the John Templeton Foundation.

### Appendix A: Quasiprobability distributions and characteristic functions

For the completeness and clarity of our presentation, here we give a few well-known formulas relating the quantities given in Tab. II, as derived by Cahill and Glauber [53]. This approach is a generalization of the standard Wigner and Glauber formalisms.

The Cahill-Glauber  $s$ -parametrized (or  $s$ -ordered) quasiprobability distribution (QPD, quasidistribution),  $\mathcal{W}^{(s)}(\alpha)$  for an  $N$ -mode bosonic state  $\hat{\rho}$  can be defined for a real parameter  $s \in [-1, 1]$  as

$$\mathcal{W}^{(s)}(\alpha) = \text{Tr} \left[ \hat{\rho} \hat{T}^{(s)}(\alpha) \right], \quad (\text{A1})$$

which is the mean value of the operator  $\hat{T}(\alpha)$  defined as

the Fourier transform,

$$\hat{T}^{(s)}(\alpha) = \int \hat{D}^{(s)}(\beta) \exp \left( \sum_n \alpha_n \beta_n^* - \text{c.c.} \right) d^2 \beta', \quad (\text{A2})$$

of the  $s$ -parametrized multimode displacement operator given by

$$\begin{aligned} \hat{D}^{(s)}(\beta) &= \prod_n \hat{D}^{(s)}(\beta_n) \\ &= \prod_n \exp \left( \beta_n \hat{a}_n^\dagger - \beta_n^* \hat{a}_n + \frac{s}{2} |\beta_n|^2 \right). \end{aligned} \quad (\text{A3})$$

Here,  $\hat{a}_n$  ( $\hat{a}_n^\dagger$ ) is the bosonic annihilation (creation) operator for the  $n$ -th mode ( $n = 1, 2, \dots, N$ ). The complex multivariable  $\alpha \equiv \{\alpha_n\} = (\alpha_1, \alpha_2, \dots, \alpha_N)$  is applied here as in Eq. (1), and, analogously  $\beta \equiv \{\beta_n\} = (\beta_1, \beta_2, \dots, \beta_N)$ . The symbol c.c. denotes the complex conjugate term, and the integration is performed over  $d^2 \beta' \equiv d^2 \{\beta_n / \pi\} = \pi^{-N} \prod_n d^2 \beta_n = \pi^{-N} \prod_n d(\text{Re} \beta_n) d(\text{Im} \beta_n)$ .

In the special cases for  $s = 1, 0, -1$ , the QPD  $\mathcal{W}^{(s)}(\alpha)$  reduces to the popular Glauber-Sudarshan  $P$ , Wigner  $W$ , and Husimi  $Q$  functions corresponding to the normal, symmetric, and antinormal orderings, respectively. Our analysis in the paper is focused on the normally and symmetrically-ordered functions. We recall that the standard definition of nonclassicality is based on the non-positivity of the  $P$  function.

The statistical operator  $\hat{\rho}$  corresponding to a given QPD can be calculated as follows

$$\hat{\rho} = \int \mathcal{W}^{(s)}(\alpha) \hat{T}^{(-s)}(\alpha) d^2 \alpha', \quad (\text{A4})$$

which, in the special case for  $s = 1$  reduces to Eq. (1) describing the  $P$  representation of a given state  $\hat{\rho}$ .

The  $N$ -mode  $s$ -parameterized characteristic function  $\mathcal{C}^{(s)}(\beta)$  for a given state  $\hat{\rho}$  can be defined as

$$\mathcal{C}^{(s)}(\beta) = \text{Tr} \left[ \hat{\rho} \hat{D}^{(s)}(\beta) \right], \quad (\text{A5})$$

which is the mean value of the multimode displacement operator  $\hat{D}^{(s)}(\beta)$ . We recall that our description of nonclassicality and entanglement is based on two special cases of these characteristic functions. Specifically, the normal characteristic function  $\mathcal{C}_N$ , defined in Eq. (7), is the special case of Eq. (A5) for  $s = 1$  assuming two-mode ( $N = 2$ ) field. While the symmetric characteristic function  $\mathcal{C}_S$  is given by Eq. (A5) for  $s = 0$  and  $N = 2$ .

For Gaussian states, which are solely analyzed in this paper, the characteristic function  $\mathcal{C}^{(s)}(\beta)$  can uniquely be defined via the covariance matrices, which are given by Eq. (10) for normal ordering ( $s = 1$ ) and by Eq. (17) for symmetric ordering ( $s = 0$ ) for a two-mode case.

By comparing the definitions in Eqs. (A1) and (A5), it is easy to conclude that the  $s$ -parameterized QPD and characteristic function for any  $s \in [-1, 1]$  are related via



the Fourier transform, i.e.,

$$\mathcal{W}^{(s)}(\boldsymbol{\alpha}) = \int \mathcal{C}^{(s)}(\boldsymbol{\beta}) \prod_n \exp(\alpha_n \beta_n^* - \alpha_n^* \beta_n) d^2 \boldsymbol{\beta}', \quad (\text{A6})$$

$$\mathcal{C}^{(s)}(\boldsymbol{\beta}) = \int \mathcal{W}^{(s)}(\boldsymbol{\alpha}) \prod_n \exp(\alpha_n^* \beta_n - \alpha_n \beta_n^*) d^2 \boldsymbol{\alpha}', \quad (\text{A7})$$

where the integration over  $d^2 \boldsymbol{\alpha}'$  is defined analogously to  $d^2 \boldsymbol{\beta}'$ , as in Eq. (A2). The normalization conditions are as follows

$$\int \mathcal{W}^{(s)}(\boldsymbol{\alpha}) d^2 \boldsymbol{\alpha}' = \mathcal{C}^{(s)}(\boldsymbol{\beta} = \mathbf{0}) = 1. \quad (\text{A8})$$

The relation between the QPDs  $\mathcal{W}^{(s_1)}(\boldsymbol{\alpha})$  and  $\mathcal{W}^{(s_2)}(\boldsymbol{\alpha})$ , assuming  $s_2 < s_1$ , is simply given by

$$\begin{aligned} \mathcal{W}^{(s_2)}(\boldsymbol{\alpha}) &= \left( \frac{2}{s_1 - s_2} \right)^M \int \mathcal{W}^{(s_1)}(\boldsymbol{\beta}) \\ &\times \exp \left( -\frac{2}{s_1 - s_2} \sum_n |\alpha_n - \beta_n|^2 \right) d^2 \boldsymbol{\beta}' \quad (\text{A9}) \end{aligned}$$

This means that the QPD  $\mathcal{W}^{(s_2)}(\boldsymbol{\alpha})$  with any parameter  $s_2 \in [-1, 1]$  can easily be obtained by mixing the  $P$  function (corresponding to  $s_1 = 1$ ) with the proper amount of Gaussian noise. The relation between the characteristic functions corresponding to different parameters  $s_1$  and  $s_2$  reads as

$$\mathcal{C}^{(s_2)}(\boldsymbol{\beta}) = \mathcal{C}^{(s_1)}(\boldsymbol{\beta}) \exp \left( \frac{s_2 - s_1}{2} \sum_n |\beta_n|^2 \right). \quad (\text{A10})$$

It is valid for any  $s_1, s_2 \in [-1, 1]$ , contrary to the analogous relation in Eq. (A9) for the QPDs. We applied Eq. (A10) to calculate the symmetrically-ordered characteristic function  $C_S \equiv \mathcal{C}^{(0)}$  from the normally-ordered characteristic function  $C_N \equiv \mathcal{C}^{(1)}$ , given by Eq. (7), for two-mode states.

- 
- [1] A. Einstein, “Über einen die Erzeugung und Verwandlung des Lichtes betreffenden heuristischen Gesichtspunkt,” *Ann. Phys.* **17**, 132 (1905).
  - [2] A. Einstein, B. Podolsky, and N. Rosen, “Can quantum-mechanical description of physical reality be considered complete?” *Phys. Rev.* **47**, 777 (1935).
  - [3] E. Schrödinger, “Die gegenwärtige Situation in der Quantenmechanik,” *Naturwissenschaften* **23**, 807 (1935).
  - [4] J. Peřina, Z. Hradil, and B. Jurčo, *Quantum Optics and Fundamentals of Physics* (Kluwer, Dordrecht, 1994).
  - [5] L. Mandel and E. Wolf, *Optical Coherence and Quantum Optics* (Cambridge University Press, Cambridge, 1995).
  - [6] R. J. Glauber, *Quantum Theory of Optical Coherence: Selected Papers and Lectures* (Wiley-VCH, Weinheim, 2007).
  - [7] V. Dodonov and V. Man’ko, *Theory of Nonclassical States of Light* (Taylor & Francis, New York, 2003).
  - [8] W. Vogel and D. Welsch, *Quantum Optics* (Wiley-VCH, Weinheim, 2006).
  - [9] J. Peřina, *Quantum Statistics of Linear and Nonlinear Optical Phenomena* (Kluwer, Dordrecht, 1991).
  - [10] R. J. Glauber, “Coherent and incoherent states of the radiation field,” *Phys. Rev.* **131**, 2766 (1963).
  - [11] E. C. G. Sudarshan, “Equivalence of semiclassical and quantum mechanical descriptions of statistical light beams,” *Phys. Rev. Lett.* **10**, 277 (1963).
  - [12] T. Richter and W. Vogel, “Nonclassicality of quantum states: A hierarchy of observable conditions,” *Phys. Rev. Lett.* **89**, 283601 (2002).
  - [13] A. Miranowicz, M. Bartkowiak, X. Wang, Y.-X. Liu, and F. Nori, “Testing nonclassicality in multimode fields: A unified derivation of classical inequalities,” *Phys. Rev. A* **82**, 013824 (2010).
  - [14] M. Bartkowiak, A. Miranowicz, X. Wang, Y. X. Liu, W. Leoński, and F. Nori, “Sudden vanishing and reappearance of nonclassical effects: General occurrence of finite-time decays and periodic vanishings of nonclassicality and entanglement witnesses,” *Phys. Rev. A* **83**, 053814 (2011).
  - [15] A. Allevi, M. Lamperti, M. Bondani, J. Peřina Jr., V. Michálek, O. Haderka, and R. Machulka, “Characterizing the nonclassicality of mesoscopic optical twin-beam states,” *Phys. Rev. A* **88**, 063807 (2013).
  - [16] W. Vogel, “Nonclassical correlation properties of radiation fields,” *Phys. Rev. Lett.* **100**, 013605 (2008).
  - [17] S. Ryl, J. Sperling, E. Agudelo, M. Mraz, S. Köhnke, B. Hage, and W. Vogel, “Unified nonclassicality criteria,” *Phys. Rev. A* **92**, 011801(R) (2015).
  - [18] O. Haderka, J. Peřina Jr., M. Hamar, and J. Peřina, “Direct measurement and reconstruction of nonclassical features of twin beams generated in spontaneous parametric down-conversion,” *Phys. Rev. A* **71**, 033815 (2005).
  - [19] J. Peřina Jr., M. Hamar, V. Michálek, and O. Haderka, “Photon-number distributions of twin beams generated in spontaneous parametric down-conversion and measured by an intensified CCD camera,” *Phys. Rev. A* **85**, 023816 (2012).
  - [20] J. Peřina Jr., O. Haderka, V. Michálek, and M. Hamar, “State reconstruction of a multimode twin beam using photodetection,” *Phys. Rev. A* **87**, 022108 (2013).
  - [21] C. T. Lee, “Higher-order criteria for nonclassical effects in photon statistics,” *Phys. Rev. A* **41**, 1721–1723 (1990).
  - [22] A. Verma and A. Pathak, “Generalized structure of higher order nonclassicality,” *Phys. Lett. A* **374**, 1009 (2010).
  - [23] C. K. Hong, Z. Y. Ou, and L. Mandel, “Measurement of subpicosecond time intervals between two photons by interference,” *Phys. Rev. Lett.* **59**, 2044 (1987).
  - [24] S. L. Braunstein, “Squeezing as an irreducible resource,” *Phys. Rev. A* **71**, 055801 (2005).
  - [25] G. Adesso, A. Serafini, and F. Illuminati, “Multipartite entanglement in three-mode Gaussian states of continuous-variable systems: Quantification, sharing structure, and decoherence,” *Phys. Rev. A* **73**, 032345 (2006).

- (2006).
- [26] G. Vidal and R. F. Werner, “Computable measure of entanglement,” *Phys. Rev. A* **65**, 032314 (2002).
  - [27] M. B. Plenio, “Logarithmic negativity: A full entanglement monotone that is not convex,” *Phys. Rev. Lett.* **95**, 090503 (2005).
  - [28] R. Horodecki, P. Horodecki, M. Horodecki, and K. Horodecki, “Quantum entanglement,” *Rev. Mod. Phys.* **81**, 865 (2009).
  - [29] Asher Peres, “Separability criterion for density matrices,” *Phys. Rev. Lett.* **77**, 1413 (1996).
  - [30] P. Horodecki, “Separability criterion and inseparable mixed states with positive partial transposition,” *Phys. Lett. A* **232**, 333 (1997).
  - [31] P. Marian and T. A. Marian, “Bures distance as a measure of entanglement for symmetric two-mode Gaussian states,” *Phys. Rev. A* **77**, 062319 (2008).
  - [32] J. K. Asbóth, J. Calsamiglia, and H. Ritsch, “Squeezing as an irreducible resource,” *Phys. Rev. Lett.* **94**, 173602 (2005).
  - [33] M. Brunelli, C. Benedetti, S. Olivares, A. Ferraro, and M. G. A. Paris, “Single- and two-mode quantumness at a beam splitter,” *Phys. Rev. A* **91**, 062315 (2015).
  - [34] A. Miranowicz, K. Bartkiewicz, A. Pathak, J. Peřina, Y.N. Chen, and F. Nori, “Statistical mixtures of states can be more quantum than their superpositions: Comparison of nonclassicality measures for single-qubit states,” *Phys. Rev. A* **91**, 042309 (2015).
  - [35] A. Miranowicz, K. Bartkiewicz, N. Lambert, Y.N. Chen, and F. Nori, “Increasing relative nonclassicality quantified by standard entanglement potentials by dissipation and unbalanced beam splitting,” *Phys. Rev. A* **92**, 062314 (2015).
  - [36] I. I. Arkhipov, J. Peřina Jr., J. Peřina, and A. Miranowicz, “Comparative study of nonclassicality, entanglement, and dimensionality of multimode noisy twin beams,” *Phys. Rev. A* **91**, 033837 (2015).
  - [37] W. Vogel and J. Sperling, “Quantum optics in the phase space,” *Phys. Rev. A* **89**, 052302 (2014).
  - [38] W. Ge, M. E. Tasgin, and M. S. Zubairy, “Conservation relation of nonclassicality and entanglement for Gaussian states in a beam splitter,” *Phys. Rev. A* **92**, 052328 (2015).
  - [39] I. Arkhipov, J. Peřina Jr., J. Svozilík, and A. Miranowicz, “Nonclassicality invariant of general two-mode Gaussian states,” *Sci. Rep.* **6**, 26523 (2016).
  - [40] M. A. Nielsen and I. L. Chuang, *Quantum Computation and Quantum Information* (Cambridge University Press, Cambridge, 2000).
  - [41] E. S. Polzik, J. Carri, and H. J. Kimble, “Spectroscopy with squeezed light,” *Phys. Rev. Lett.* **68**, 3020 (1992).
  - [42] T. C. Ralph and P. K. Lam, “Teleportation with bright squeezed light,” *Phys. Rev. Lett.* **81**, 5668 (1998).
  - [43] F. Wolfgramm, A. Ceré, F. A. Beduini, A. Predojević, M. Koschorreck, and M. W. Mitchell, “Squeezed-light optical magnetometry,” *Phys. Rev. Lett.* **105**, 053601 (2010).
  - [44] J. Peřina, Jr. and J. Peřina, “Quantum statistics of nonlinear optical couplers,” *Prog. Opt.* **41**, 361 (2000).
  - [45] J. Peřina and J. Křepelka, “Joint probability distribution and entanglement in optical parametric processes,” *Opt. Commun.* **284**, 4941 (2011).
  - [46] R. Simon, “Peres-Horodecki separability criterion for continuous variable systems,” *Phys. Rev. Lett.* **84**, 2726 (2000).
  - [47] P. Marian, T. A. Marian, and H. Scutaru, “Inseparability of mixed two-mode Gaussian states generated with a SU (1,1) interferometer,” *Journal of Physics A: Mathematical and General* **34**, 6969 (2001).
  - [48] S. Olivares, “Quantum optics in the phase space,” *Eur. Phys. J. Special Topics* **203**, 3 (2012).
  - [49] D. N. Klyshko, “Quantum optics: Quantum, classical, and metaphysical aspects,” *Physics-Uspekhi* **37**, 1097 (1994).
  - [50] T. Sh. Iskhakov, K. Yu. Spasibko, and M. V. Chekhova, “Macroscopic Hong-Ou-Mandel interference,” *New J. Phys.* **15**, 093036 (2013).
  - [51] M. G. A. Paris, “Joint generation of identical squeezed states,” *Phys. Lett. A* **225**, 28 (1997).
  - [52] A. Lukš, V. Peřinová, and J. Peřina, “Principal squeezing of vacuum fluctuations,” *Opt. Commun.* **67**, 149 (1988).
  - [53] K. E. Cahill and R. J. Glauber, “Ordered expansions in boson amplitude operators,” *Phys. Rev.* **177**, 1857 (1969).